Atmos. Meas. Tech. Discuss., https://doi.org/10.5194/amt-2018-329
Manuscript under review for journal Atmos. Meas. Tech.
Discussion started: 4 October 2018

Atmospheric Measurement Techniques Discussions

Characterization of lower-cost medium precision atmospheric CO_2 monitoring systems for urban areas using commercial NDIR sensors

Emmanuel Arzoumanian[1], Felix R. Vogel[1,2*], Ana Bastos[1], Bakhram Gaynullin[3], Olivier Laurent[1], Michel Ramonet[1] and Philippe Ciais[1*]

1 LSCE/IPSL, CEA-CNRS-UVSQ, Universite Paris-Saclay, Gif-Sur-Yvette, France
2 Climate Research Division, Environment and Climate Change Canada, Toronto, Canada
3 SenseAir AB, Delsbo, Sweden

* Corresponding authors: Felix.Vogel@canada.ca and Philippe.Ciais@lsce.ipsl.fr

Abstract:

CO_2 emission estimates from urban areas can be obtained with a network of in-situ instruments measuring atmospheric CO_2 combined with high-resolution (inverse) transport modeling. The distribution of CO_2 emissions being highly heterogeneous in space and variable in time in urban areas, gradients of atmospheric CO_2 need to be measured by numerous instruments placed at multiple locations around and possibly within these urban areas, which calls for the development of lower-cost medium precision sensors to allow a deployment at required densities. Medium precision is here set to be a random error (uncertainty) on hourly measurements of ±1 ppm or less, a precision requirement based on previous studies of network design in urban areas. Here we present tests of a HPP commercial NDIR sensors manufactured by Senseair AB performed in the laboratory and at actual field stations, the latter for CO_2 concentration in the Paris area. The lower-cost medium precision sensors are shown to be sensitive to atmospheric pressure and temperature conditions. The sensors respond linearly to CO_2 when measuring calibration tanks, but the regression slope between measured and true CO_2 differs between individual sensors and changes with time. In addition to pressure and temperature variations, humidity impacts the measurement of CO_2, all causing systematic errors. In the field, an empirical calibration strategy is proposed based on parallel measurements with the lower-cost medium precision sensors and a high-precision instrument cavity ring-down instrument during 6 month. This empirical calibration method consists of using a multiple regression approach to create a model of the errors defined as the difference of CO_2 measured by the lower-cost medium precision sensors relative to a calibrated high-precision instrument, based on predictors of air temperature, pressure and humidity. This error model shows good performances to explain the observed drifts of the lower-cost medium precision sensors on time scales of up to 1-2months when trained against 1-2 weeks of high-precision instrument time series. Residual errors are contained within the ±1 ppm target, showing the feasibility to use networks of HPP instruments for urban CO_2 networks, provided that they could be regularly calibrated against one anchor reference high-precision instrument.

1. Introduction

Urban areas cover only a small portion (< 3 %) of the land surface but account for about 70% of fossil fuel CO_2 emissions (Liu et al. 2014, Seto et al. 2014). Uncertainties of fossil fuel CO_2 emissions from inventories based on statistics of fuel amounts and/or energy consumption are on the order of 5% for OECD countries and up to 20% in other countries (Andres et al. 2014) but they are larger in the case of cities (Breon et al. 2015, Wu et al. 2016). Further, in many cities of the world, there are no emission inventories available. The need to provide more reliable

Atmos. Meas. Tech. Discuss., https://doi.org/10.5194/amt-2018-329
Manuscript under review for journal Atmos. Meas. Tech.
Discussion started: 4 October 2018

Atmospheric Measurement Techniques Discussions

information on emission and emission trends has prompted research projects seeking to provide estimates of GHG budget cities, power plants and industrial sites, based on in situ measurements made at surface stations (Staufer et al. 2016, Lauvaux et al. 2016, Verhulstet al. 2017), aircraft campaigns around emitting locations Mays et al. 2009, Cambaliza et al. 2014) and satellite imagery (Broquet et al. 2017, Nassar et al. 2017). Although sampling strategies and measurement accuracies differ between these approaches, the commonly used principle is to measure atmospheric CO_2 mixing ratio gradients at stations between the upwind and downwind vicinity of an emitting area and infer the emissions that are consistent with those CO_2 gradients and their uncertainties, using an atmospheric transport model. This approach is known as atmospheric CO_2 inversion or as a "top-down" estimate.

Inversion studies from Paris, France attempting to constrain CO_2 emissions from measurements of CO_2 mixing ratios at four stations located around the city along the dominant wind direction, have pointed out that the fast mixing by the atmosphere and the complex structure of urban CO_2 emissions requires high resolution atmospheric transport models, and continuous measurements of the atmosphere to select gradients induced by emission plumes (Broquet et al. 2015, Wu et al. 2016) that can be captured at the scale of the model.

With four stations, only the CO_2 emissions from the Paris megacity could be retrieved with an accuracy of ≈20% on monthly budgets (Wu et al. 2016). A denser network of stations would help to obtain more information on the spatial details of CO_2 emissions. A network design study by Wu et al. 2016 for the retrieval of CO_2 emissions per sector for the Paris Megacity has shown that with 10 stations measuring CO_2 with 1 ppm accuracy on hourly time-steps, the error of the annual emission budget could be reduced down to a 10% uncertainty. Wu et al. 2016 furthermore found that for a more detailed separation of emissions into different sectors, more stations were needed, on the order of 70 stations to be able to separate road transport from residential CO_2 emissions. This inversion based on pseudo-data allowed estimating total CO_2 emissions with a better accuracy than 10% and emissions of most major source sectors (building, road energy) with an accuracy better than 20%. Another urban network design study over the San Francisco Bay area reached a similar conclusion, i.e. that in-situ CO_2 measurements from 34 stations with 1 ppm accuracy at an hourly resolution could estimate weekly CO_2 emissions from the city area with less than 5 % error (Turner et al. 2016).

In the studies from Wu et al. 2016 and Turner et al. 2016, the additional number of atmospheric CO_2 measurement stations rather than the individual accuracy of each measurement helped to constrain emissions, provided that CO_2 observation errors have random errors of less than 1 ppm on hourly measurements, uncorrelated in time, and in space between stations. Therefore, we will adopt here a 1 ppm uncertainty on hourly CO_2 data as the target performance for new urban lower-cost medium precision CO2 sensors.

Today, the continuous CO_2 gas analyzers used for continental scale observing systems like ICOS (https://www.icos-ri.eu/), NOAA (https://www.esrl.noaa.gov/gmd/) or ECCC (https://www.canada.ca/en/environment-climate-change.html) follow the WMO/GAW guidelines and are at least ten times more precise than our target of 1 ppm, but are also quite expensive. Because for urban inversions, the number of instruments is more important than their individual precision, if low-cost sensors could be produced with the specifications of 1 ppm random error, significant expansion of urban networks could be achieved at an acceptable cost.

Recently, inexpensive sensors, measuring trace gases, particulate matter, as well as traditional meteorological variables, using various technologies and accuracy have become commercially available. Evaluation and implementation of these sensors is quite promising (Eugster and Kling 2012, Holstius et al. 2014, Piedrahita et al. 2014, Young et al. 2014, Wang et al. 2015, Martin et al. 2017). With the advent of low cost mid-IR light sources and detectors, different non-dispersive infrared (NDIR) CO_2 sensors have become commercially available.

In this study, we present the development and stability tests of an inexpensive instrument to measure CO_2 based on controlling parameters for ambient air using a Senseair HPP NDIR

sensor for CO_2 measurements (Hummelgard et al. 2015). The instrument sensitivities to ambient air temperature, pressure and water vapor content are assessed in laboratory experiments and climate chambers tests. Then, the instrument linearity is evaluated against a suite of CO_2 reference gases calibrated from 330 to 1000 ppm. The calibrated low-cost medium precision (LCMP) instruments are then compared to highly precise CRDS instruments (G2401, Picarro Inc, Santa Clara, USA).
Lastly we present the time series of ambient air CO_2 measurements in the Paris region environment. The time series are compared to co-located CRDS-based CO_2 observations, and Empirical corrections to the HPP-based instrument are proposed based on CO_2 and meteorological variables. These corrections established during a period of 1 or 2 weeks are used to estimate the drift of the HPP-instrument on time scales of up to a month and a half.

2. Sensor integration

2.1. HPP sensor

The HPP (High-Performance Platform) NDIR CO_2 sensor from SenseAir AB (Delsbo, Sweden) is a commercially available lower-cost system (Hummelgard et al. 2015). The main components of this sensor are: an infrared source (lamp), a sample chamber (ca. 1m optical path length), a light filter and an infrared detector. The gas in the sample chamber causes absorption of specific wavelengths (Hummelgard et al. 2015) according to the Beer–Lambert law, and the attenuation of light in these wavelengths is measured by a detector to determine the gas mixing ratio. The detector has an optical filter in front of it that eliminates all light except the wavelength that the selected gas molecules can absorb. The HPP has a factory pre-calibrated CO_2 measurement range of 0 to 1000 ppm. The HPP sensor itself uses ca. 0.6 W and requires 12 VDC and has a life expectancy superior to 15 years according to the manufacturer.
Three generation of HPP sensors were built by SenseAir AB (Delsbo, Sweden), in this manuscript we only report on the tests carried out on the latest generation (HPP3) being the most performant among the HPP sensors family. Previous HPP versions were used for more short-term airborne measurements, for example in the COCAP system (Kunz et al. 2017) and were found to have an accuracy of 1-1.2 ppm during short-term mobile campaigns.

A number of technical improvements have been made for the new (third) HPP generation described here:

- Simple interface through USB connection and the development of a new software made data transfer easier, quicker and more efficient
- Improved temperature stability due to 6 independent heaters dispatched inside the unit.
- The sample cell design is optimized in order to match with targeted production costs. The optical length was slightly reduced to 95cm so the related alcohol sensor platform could be used to benefit from any development of this product line.
- To improve long-term drift the sensor is equipped with new electronics and the IR sources were preconditioned prior to shipment.
- The improved second version of HPP3 (HPP3.2) sensors was equipped with a pressure sensor (LPS331AP - ST Microelectronics, Switzerland) to allow real-time corrections.
- Leakage problems impact are minimized since the third generation sensor works in a high pressure mode. A pump is thus needed upstream of the sensor inlet in order to create a high pressure in the measurement cell.

Atmos. Meas. Tech. Discuss., https://doi.org/10.5194/amt-2018-329
Manuscript under review for journal Atmos. Meas. Tech.
Discussion started: 4 October 2018

Atmospheric Measurement Techniques Discussions

Different sensors from two versions of HPP3 were tested and used in this study, that is, three sensors from a first version (HPP3.1) named S1.1, S1.2 and S1.3, and three others from the second better version (HPP3.2) named S2.1, S2.2 and S2.3.

2.2. Portable integrated instrument

The HPP sensors were integrated into a custom-built portable instrument suitable to perform in-situ CO_2 measurements on ambient air. The instrument is composed of the HPP CO_2 sensor, temperature (T) and relative humidity (RH) sensors. For pressure, a LPS331AP (ST Microelectronics, Switzerland) sensor was added inside the HPP3.2 sensors. LPS331AP has a pressure range of 0.26 to 1.26 atm, a high resolution mode of $2x10^{-5}$ atm Root Mean Square (RMS) and low power consumption (30 µA for high resolution mode). For humidity and temperature, a DHT22 sensor (Adafruit, USA) was added in the instrument enclosure and connected through an I2C interfaces. The accuracy of the sensor is ±2% RH and ±0.5°C. Its range is 0-100 %RH and -40 to +80°C, respectively.
A Raspberry Pi3 (RPi3) (Raspberry Pi Foundation, 2015) is used to collect the data of all sensors. The RPi3 is a small (85x56 mm) processor running with Rasbian OS which is a Linux distribution. It has 40-pin extended GPIO which allows connecting number of sensors, 4 USB2 ports, BCM43438 wireless LAN and Bluetooth low energy on board.
A 7'' touch screen monitor is connected via an adapter board which handles power and signal conversion. To be able to flush the measurement cell a diaphragm micro pump (GardnerDenverThomas, USA, Model 1410VD/1.5/E/BLDC/12V) with an external speed adaptor is used. A 12 V power supply is sufficient to power the integrated package. An image of the complete portable instrument package is available in Figure1.

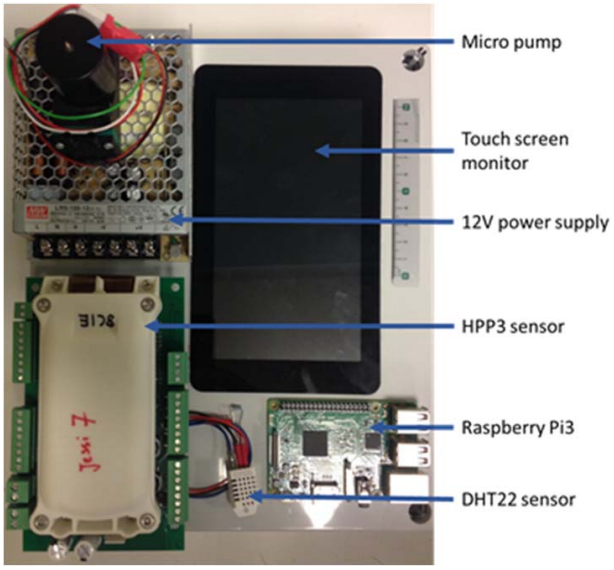

Figure 1: Components of the portable instrument on the top of its box.

3. Methods

Atmos. Meas. Tech. Discuss., https://doi.org/10.5194/amt-2018-329
Manuscript under review for journal Atmos. Meas. Tech.
Discussion started: 4 October 2018

Atmospheric Measurement Techniques Discussions

NDIR sensors are sensitive to IR light absorption by CO_2 in the air contained in their optical cell, but the retrieval of CO_2 concentration to the desired accuracy of 1 ppm is made difficult by sensitivities to temperature, pressure and humidity. Therefore, these parameters should be controlled as much as possible, and their sensitivities characterized, to calculate CO_2. A series of tests were carried out to characterize the HPP3.1 (S1.1, S1.2, S1.3) and HPP3.2 (S2.1, S2.2, S2.3) performances and sensitivities to CO_2, T, P and RH. Firstly, temperature, pressure and CO_2 sensitivities were determined in laboratory experiments. Then, field measurements were conducted with an accurate instrument (Picarro, USA, G2401) measuring the same air than the HPP; The G2401 accuracy is estimated to be below 0.05 ppm (Rella et al., 2013). Table1 summarizes all laboratory tests and field tests measurements, which are presented upon in this section. The general test setup for the experiments can be seen in Figure 3.

Name	Purpose	Location	Air measured	Parameter	Range of T (°C) and P (atm)	Range of [CO2] in air (ppm)	Range of [CO2] in Cal. Cylinders (ppm)	Duration (days)	Sensors tested
PT1	Correlation between [CO2] and P / T	plastic chamber (Saclay)	Calibration cylinders	T, P	16-32 and 0.965-1.025	N/A	420 to 450	3	S1.1, S1.2, S1.3
PT2	Correlation between [CO2] and P / T	PIT climate chamber (Guyancourt)	Calibration cylinders	T, P	-2 to 35 and 0.75 to 0.95	N/A	420 to 450	5	S2.1, S2,2, S2.3
DA1	Test calibration frequency	Laboratory (Saclay)	Calibration cylinders and dried outside air	T , P, H2O, [CO2] from CRDS	24 to 31 and 0.996 to 1.010	417 to 575	330 to 1000	48	S1.1, S1.2, S1.3
WA2-1	Test calibration frequency	Laboratory (Saclay)	Outside air	T, P, H2O, [CO2] from CRDS	25 to 27 and 0.999 to 1.008	389 to 508	N/A	45	S2.2, S2.3
WA2-2	Test calibration frequency	Laboratory (Jussieu)	Outside air	T, P, H2O, [CO2] from CRDS	29 to 31 and 0.993 to 1.021	393 to 521	N/A	60	S2.1

Table 1: Summary of all laboratory tests.

3.1. Laboratory tests

3.1.1. Sensitivity to temperature and pressure variations

Two series of temperature and pressure sensitivity tests (PT1, PT2) were realized in a closed chamber with controlled T and P for the HPP3.1 and HPP3.2 sensors. These tests are for assessing the linearity of the response of each sensor to CO_2 for different pressure and temperature conditions. For the HPP3.1 sensors, an internal pressure compensation does not exist, but the HPP3.2 series includes a pressure sensor together with a compensation algorithm which normalizes measured CO_2 mixing ratios according to ambient pressure (Gaynullin et al. 2016).

In test PT1 (table1), three HPP3.1 sensors were put in a simple plastic chamber and exposed to pressure changes ranging from 0.965 to 1.025 atm, and temperature ranges of 16 to 32 °C. Pressure and temperature were measured by a high-precision pressure sensor (Keller, Germany, Series 33x, 0.01% precision).

Atmos. Meas. Tech. Discuss., https://doi.org/10.5194/amt-2018-329
Manuscript under review for journal Atmos. Meas. Tech.
Discussion started: 4 October 2018

Atmospheric Measurement Techniques Discussions

In test PT2, three HPP3.2 sensors were placed inside a dedicated temperature and pressure chamber at the Plateforme d'Integration et de Tests at OVSQ Guyancourt, France (PIT) where a much larger range of T and P variations could be applied. During each T, P test, four calibration cylinders with dry air CO_2 mixing ratios from 420 to 450 ppm were measured by all the HPP3.2 sensors for a period of approximately 120 hours for each cylinder. In the PIT chamber, temperatures was varied from -2 to 35 °C with linear rates of change of 1 °C/hour keeping pressure constant at a value of 0.95 atm. Pressure was varied from 0.95 to 0.75 atm with an increment of 5.10^{-2} atm, being regulated with a primary pump, with temperature fixed at 15°C.

3.1.2. Calibration of CO_2 variations measured by the sensors for dry and wet air

These experiments were performed to evaluate the response of HPP sensors to CO_2 changes in ambient air. Two modes of operations have been tested i.e. using either a dried or an undried gas streams, described as follows.

Dry air experiments

Water vapor is known to interfere with CO_2 measurements, in particular for NDIR sensors. It is thus important to determine the sensitivity of the sensors to CO_2 under the best possible conditions, that is, dry air. In test DA1 (Table 2) different HPP sensors were flushed with the same dry ambient air, passed through a Nafion dryer (PermaPure, USA, Model MD-070). Online CRDS measurement confirmed that H_2O was reduced to trace amounts, i.e. 0.05 ±0.05 % H_2O. HPP3.1 sensors S1.1, S1.2, S1.3 were tested extensively during 45 days, and HPP3.2 sensors S2.1, S2.2 were tested during 12 days. No significant difference was found between the performances of both HPP versions. The experimental setup is shown in Figure 2. For the period of 45 days during spring 2016, S1.1, S1.2 and S1.3 measured dry ambient air in parallel with a co-deployed CRDS instrument (Picarro, USA, G2401). The ambient air was pumped from a sampling line fixed on the roof of the building (ca. 4 m a.g.l.) to flush the setup described in Fig. 2. In addition, four dry-air calibration cylinders (330 ppm, 375 ppm, 445 ppm and 1000 ppm of CO_2) were measured successively each 13 hours during 30 minutes (Figure 3). As the HPP responses can be slow, in order to remove memory effects, only the last 15 minutes of each calibration periods were used.

Wet air experiments

Because in the field, drying is often impractical, we also measured the HPP sensitivities to water vapor under worst-case conditions, that is both ambient air and calibration cylinders air being wet. If these sensitivities were stable over time, they could be used to correct CO_2 for the H_2O interference. For WA2-1 and WA2-2 tests, the Nafion dryer was removed from the setup.

Atmos. Meas. Tech. Discuss., https://doi.org/10.5194/amt-2018-329
Manuscript under review for journal Atmos. Meas. Tech.
Discussion started: 4 October 2018

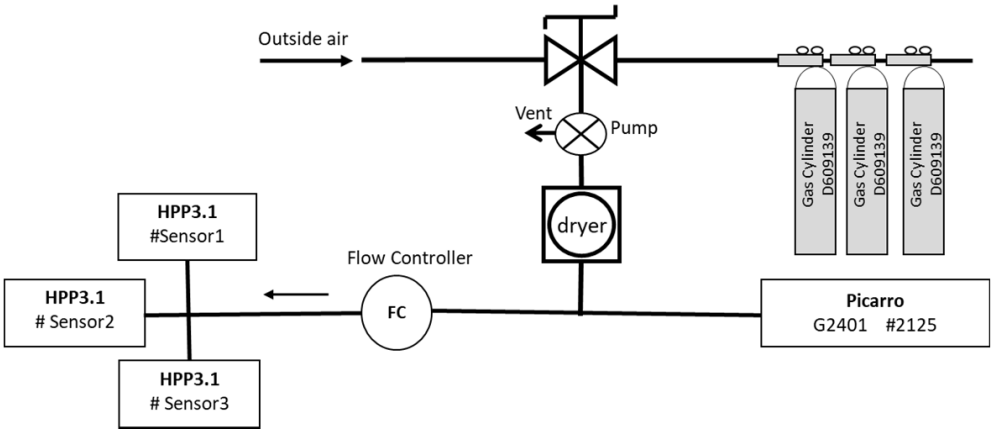

246
247

248 ***Figure 2:*** HPP3 instruments test Setup
249

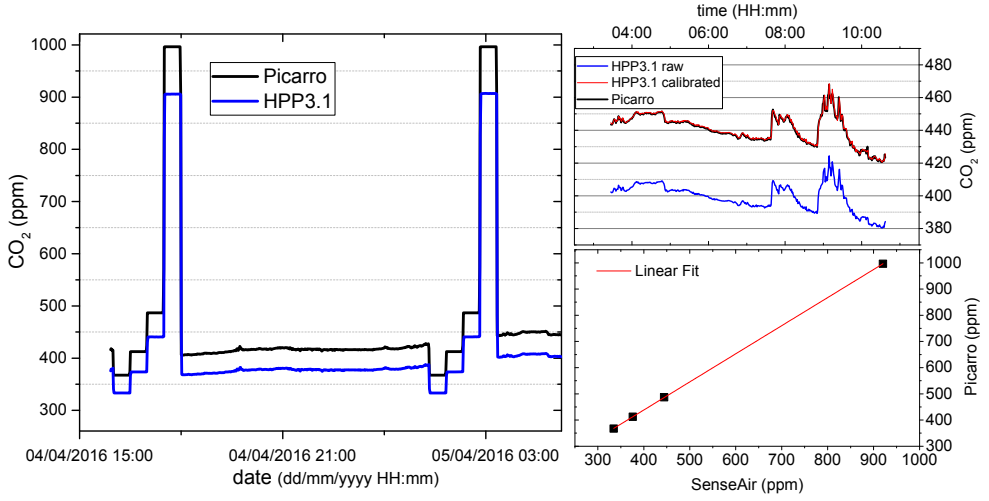

250
251 ***Figure 3:*** Left – CO_2 mixing ratios measured by S1.1 (blue) and the Picarro CRDS analyzer
252 (black). Right - calibrated mixing ratios of S1.1 (red) compared to the raw values (blue). Below:
253 Four reference gases (367 ppm, 413 ppm, 487 ppm and 997 ppm of CO_2), are used for the
254 calibration. No saturation effects are observed within our CO_2 mixing ratio range.
255
256 **3.2. Instrument calibration procedure**
257
258 **Dry air calibration**
259
260 For dry air measurements in test DA1, a linear calibration curve is used. The lower right graph of
261 Figure 3 shows that the response of the HPP3 instruments to CO_2 mixing ratio is linear (R^2 =

Atmos. Meas. Tech. Discuss., https://doi.org/10.5194/amt-2018-329
Manuscript under review for journal Atmos. Meas. Tech.
Discussion started: 4 October 2018

Atmospheric Measurement Techniques Discussions

0.95) from 330 to 1000 ppm. No saturation effects are observed within this CO_2 mixing ratio range since residuals are included in the ±1 ppm range.

Wet air calibration

Due to the high correlation of air temperature and water vapor content, we have applied a multivariate regression method, which includes all environmental variables. Indeed, if variables are corrected one at a time, an overcorrection of one of the correlated variables may occur.
Multi-linear regression is a generalization of linear regression by considering more than one variable. We used a multivariate linear regression of the form:

$$y = b + a_C x_C + a_p x_P + a_T x_T + a_w x_w + a_{xy} x_{xy} \quad (1)$$

y is the CO_2 value measured by the reference accurate instrument (CRDS), considered as the true value here. X_C is the CO_2 measured with the HPP3 instrument, with additional factors to capture the influence of the pressure *P*, the temperature *T*, the water mixing ratio *W*, the baseline drift *xy* and a baseline offset *b*. Baseline drifts are corrected by fitting a linear y=x curve in which y is incremented with time. Instrument specific coefficients for the multivariate linear regression are determined using measurements of the parameters during several days.

3.3. Field tests with urban air measurements

To assess their real-world performance of the sensors, we conducted additional tests for the HPP sensors measuring outside air under typical conditions for urban air monitoring, after the sensors were fully integrated into instruments as described in section 2.2. Three HPP3.1 instruments (S1.1, S1.2, S1.3) and two HPP3.2 instruments (S2.2, S2.3) were installed in the laboratory building of Saclay (48.7120N, 2.1462E) to measure outside air on top of the building roof. Saclay is located 20 kilometers south of the center of Paris in a low-urbanized area. In addition, one HPP3.2 instrument (S2.1) was installed to measure air on the Jussieu University campus in the center of Paris (48.8464N, 2.3566E).

3.3.1. Saclay Site

The sampling line, a 5 meter Dekabon tube with an inner tube of 0.6 cm, was fixed on the rooftop of the building at about 4 meters above the ground. The laboratory hosting the five instruments is equipped with a cooling/heating unit that was turned off most of the time so that room temperature varied between 24 and 31 °C. A CRDS (Picarro, USA, G2401) measured air from the same intake in parallel as seen in Figure 3. A diaphragm pump (KNF Lab, Germany, Model N86KN.18) was used to pump air to the five instruments, and a flow controller (Bronkhorst, France, El-Flow series) was used to regulate the air-flow distributed with a manifold to the HPP3 instruments at 500 mln min^{-1} to ensure stable experimental conditions. For dry air measurements using the HPP3.1 (48 days) an external Nafion dryer (PermaPure, USA, MD-070 series) was used to eliminate H_2O traces in the gas line during dry air experiments, while HPP3.2 were tested for 45 days. Four reference gas cylinders (330ppm, 375ppm, 445ppm and 1000 ppm of CO_2) were used and each HPP was flushed every 12 hours for 30 minutes during the dry air experiment. No calibration cylinders were used during the undried air experiment, since the calibration was based on the co-located high precision measurement with the CRDS analyzer. The mean mixing ratio of ambient CO_2 was 420 ppm and varied between 388 ppm and 575 ppm during dry air experiments and a mean of 409 ppm and varied between 389 ppm and 509 ppm during undried air experiments.

3.3.2. Jussieu site

The measurements from the HPP3.2 instrument (S2.1) in Jussieu were compared with those of a co-located CRDS (Picarro, USA, G2401). Two independent sampling lines (about 5 meter Dekabon tube with an inner tube of 0.6 cm) were used for the Picarro, and the S2.1 instrument. The air-flow into HPP3.2 instrument was regulated by the micro pump (see section 2.2) and set to 500 mln min^{-1}. At this location neither calibration cylinders nor a drying system were deployed for the HPP3.2. The measurement period was 60 days and the mean ambient CO_2 mixing ratio was 410 ppm and minute averages varying between 393 ppm and 521 ppm. Room temperature varied between 28 and 31 °C during the observation period.

4. Results

4.1. *Sensitivity to temperature and pressure variations using dried air*

4.1.1. HPP3.1 instruments tested in the simple chamber

As shown in Figures 6 and 7 linear relationships are observed between CO_2 concentrations and P, T (R^2 =0.99 with P and R^2 = 0.92 with T) in the simple chamber. Due to the limitation of experimental conditions in these simple plastic chambers, only a narrow pressure range of 0.965 to 1.020 atm and a temperature range of 16 °C to 32 °C could be tested for these instruments. Different slopes and intercepts are found for each instrument as reported in Table 2. This indicates that there is no single universal P and T calibration curve that could be determined for one instrument and used for others.

4.1.2. HPP3.2 instruments tested in the PIT chamber

The PIT tests results with P changes from 1.00 to 0.75 atm with an increment of 5.10^{-2} atm are shown in Figure 4. The top panel of the Figure 4 shows the variations of CO_2 mixing ratios due to P (from 0.5 to 1.8 ppm per 0.1 atm). Despite the built-in pressure compensation algorithm developed for HPP3.2, CO_2 and P can still co-vary with a positive (S2.1 and S2.2) or a negative (S2.3) correlation, indicating that an additional correction would be required when aiming to achieve the best possible results. Consequently, we applied a linear fit between ΔCO_2 (differences between the known mixing ratio in the cylinder and the mixing ratio measured by HPP3.2 instruments) and pressure (Figure 6). The slope and intercept obtained are then used to determine the offset due to P variations that has to be added on raw CO_2 mixing ratios reported by the HPP3.2 instruments. The lower panel of Figure 4 shows that the corrected CO_2 mixing ratios values have a root mean square deviation from the true mixing ratio in the calibration cylinder (428.6 ppm) of less than 0.02 ppm for all three HPP3.2.

Figure 5 shows the effect of temperature variations in the PIT chamber going from -2 to 35 °C (see section 3.1) on raw reported CO_2 mixing ratio of the HPP3.2 instruments. Temperature corrections are done following the same steps as for P. For the three HPP3.2, CO_2 mixing ratios are negatively correlated to T. As for the tests in the simple chamber with the HPP3.1 instruments, different linear T slopes and intercepts are observed for each HPP3.2 instrument (Figure 6) in the PIT chamber. After correction for temperature variations, we obtain corrected

Atmos. Meas. Tech. Discuss., https://doi.org/10.5194/amt-2018-329
Manuscript under review for journal Atmos. Meas. Tech.
Discussion started: 4 October 2018

Atmospheric Measurement Techniques Discussions

357 CO_2 mixing ratio values with a root mean square deviation which does not exceed 0.01 ppm
358 from the true value of the cylinder ([CO_2]=444 ppm) for the three HPP3.2 instruments.
359

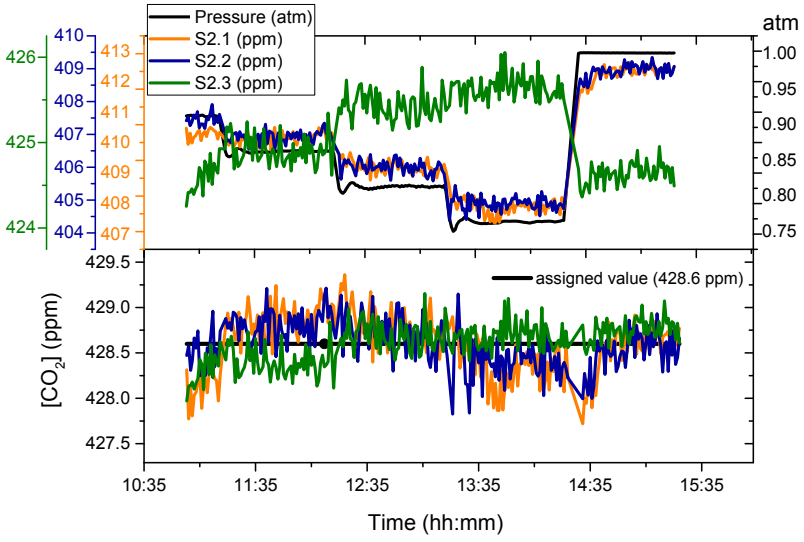

360
361 ***Figure 4:*** Upper panel – Effect of pressure variations (black) on raw CO_2 mixing ratios of three
362 HPP3.2 instruments measuring CO_2 from air from the same calibration cylinder (true value
363 =428.6 ppm), S2.1 (orange), S2.2 (blue) and S2.3 (green), please not the different y-axis scales.
364 Lower panel – Corrected CO_2 mixing ratios for HPP3.2 instruments.
365

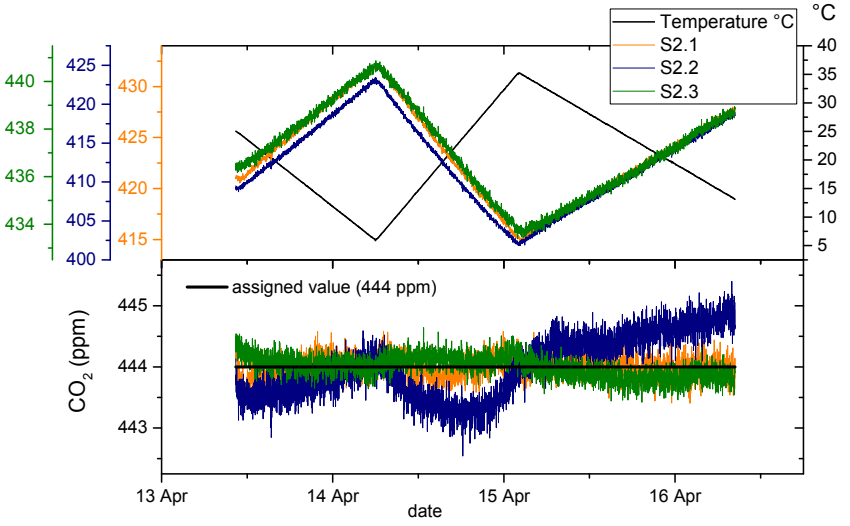

366

Atmos. Meas. Tech. Discuss., https://doi.org/10.5194/amt-2018-329
Manuscript under review for journal Atmos. Meas. Tech.
Discussion started: 4 October 2018

Atmospheric Measurement Techniques Discussions

Figure 5: Upper panel – The effect of temperature variations (black) on raw CO_2 mixing ratios of HPP3.2 instruments measuring CO_2 from air from the same calibration cylinder (true value =444 ppm), S2.1 (orange), S2.2 (blue) and S2.3 (green), please not the different y-axis scales. Lower panel – Corrected CO_2 mixing ratios for HPP3.2 instruments.

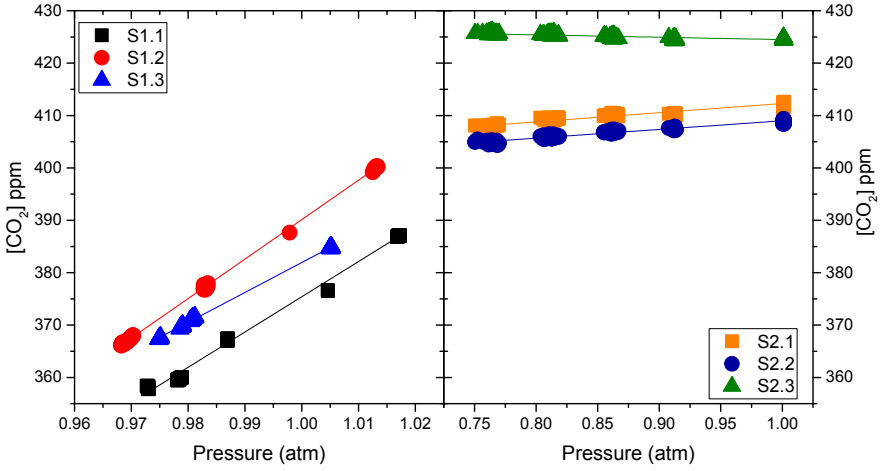

Figure 6: Linear relationship experimentally found between CO_2 mixing ratios and P for the HPP3.1 instruments (S1.1, S1.2, S1.3) (left) and for the HPP3.2 instruments (S2.1, S2.2, S2.3) (right). Note the different P range, going from 0.96 to 1.02 atm. for the HPP3.1 in the simple plastic chamber to 0.75 to 1 atm. for the HPP3.2 in the PIT chamber.

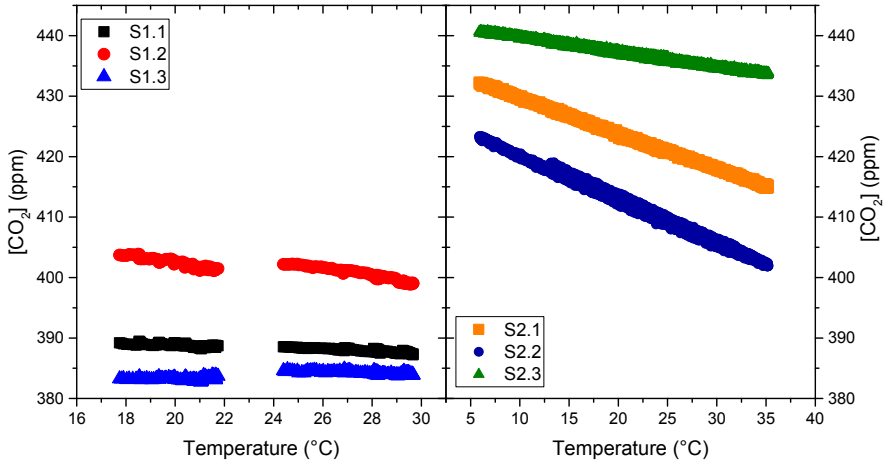

Figure 7: Linear relationships between CO_2 mixing ratios for HPP3.1 S1.1, S1.2 and S1.3 (left)

at temperature values going from 17 to 30 °C in plastic chamber, and for HPP3.2 S2.1, S2.2 and S2.3 at temperature values going from 5 to 35 °C in the PIT chamber.

Table 2 summarizes the results of the pressure and temperature tests for all the HPP3 instruments. These tests results show a sensor-specific response to P and T. A large difference of CO_2 mixing ratios sensitivity to pressure variations is observed between the two HPP3 versions. A sensitivity of 571.5 to 753.4 ppm/atm is found for the HPP3.1 versions, whereas this sensitivity ranges from -4.5 up to 17.6 ppm/atm for the newest HPP3.2 versions. The lower sensitivity among HPP3.2 prototypes is due to the pressure compensation algorithm which is included in this model. Since the pressure compensation algorithm does still not fully correct the CO_2 variations due to pressure changes, we found that it is necessary to apply a correction for pressure interferences on the CO_2 mixing ratios signal, and that is correction should be sensor specific. The CO_2 mixing ratios sensitivity to temperature variations are found to be in similar ranges for both sensors. Sensitivities of -0.3 to 0.1 ppm/°C and -0.2 to -0.7 ppm/°C are found for HPP3.1 and HPP3.2 prototypes respectively.

	Pressure			**Temperature**		
	Slope (ppm/atm)	**Intercept (ppm)**	**R^2**	**Slope (ppm/°C)**	**Intercept (ppm)**	**R^2**
S1.1	673.1 ±4.4	-297.7 ±4.3	0.94	-0.124 ±0.003	391.34 ±0.07	0.85
S1.2	753.4 ±1.1	-363.3 ±1.1	0.95	-0.29 ±0.01	408.1 ±0.2	0.80
S1.3	571.5 ±1.4	-189.5 ±1.4	0.94	0.107 ±0.004	381.2 ±0.1	0.63
S2.1	17.6 ±0.2	394. ±0.2	0.95	-0.5854 ±0.0004	435.530 ±0.01	0.99
S2.2	16.6 ±0.2	392.4 ±0.2	0.97	-0.716 ±0.001	427.31 ±0.02	0.99
S2.3	-4.5 ±0.0	429.0 ±0.0	0.75	-0.2453 ±0.0004	442.16 ±0.01	0.99

Table 2: Slopes and intercept calculated for CO_2 correction due to temperature and pressure. Sensor 1 to 3 are type HPP3.1, whereas Sensor 4 to 6 are HPP3.2.

From Figures 6 and Table 2, we see a positive correlation between CO_2 and P for five instruments (S1.1, S1.2, S1.3, S2.1 and S2.2) and a negative correlation for S2.3. In Figures 7 and Table 2, a negative correlation between CO_2 and temperature is found for 5 instruments (S1.1, S1.2, S2.1, S2.2 and S2.3) and a positive one for S1.3. After correcting for temperature and pressure, no more correlations are observed between corrected CO_2 and pressure and temperature. Corrected CO_2 mixing ratios of HPP3.2 are stable and standard errors do not exceed 0.3 ppm and 0.2 ppm for pressure and temperature corrections respectively, except for

Atmos. Meas. Tech. Discuss., https://doi.org/10.5194/amt-2018-329
Manuscript under review for journal Atmos. Meas. Tech.
Discussion started: 4 October 2018

Atmospheric Measurement Techniques Discussions

406 CO_2 mixing ratios after temperature correction for S2.2 which reaches a standard deviation
407 (STD) of 0.5 ppm. However, we do not reach the same stability after pressure and temperature
408 correction for HPP3.1 prototypes. Standard deviations of 0.9, 0.2 and 0.2 ppm are calculated for
409 S1.1, S1.2 and S1.3 respectively after pressure correction, and Standard deviations of 1.3, 2.6
410 and 1.6 ppm are determined for S1.1, S1.2 and S1.3 respectively after temperature corrections.
411 These differences between the results of the two HPP3 versions can be explained by the fact
412 that HPP3.2 prototypes had the opportunity to be tested in a sophisticated climatic chamber
413 which respects precise temperature and pressure setpoints and in which only one of the two
414 variables are modified one at a time.
415
416 **4.2. Instrument calibration and stability during continuous measurements**
417
418 Given that the instrument response to CO_2 is affected by atmospheric water vapor, we present
419 the results from dried and wet ambient air measurements separately.
420
421 ***4.2.1. Measurements of dried ambient air (test DA1)***
422
423 Four calibration cylinders were used in order to linearly calibrate the three HPP3.1 instruments
424 (see section 3.1). To assess the quality of this calibration, the RMS relative to 1-minute CO_2
425 mixing ratios from the co-located CRDS data were calculated, and shown in Figure 8. Although
426 calibration cylinders were measured each 12 hours, by ignoring deliberately some calibrations,
427 we processed the time series to re-compute CO_2 assuming a range of different time intervals
428 between two calibrations. The results shown in figure 8 are for calibrations intervals of 0.5, 6, 12,
429 19, 25, 31, 38 and 45 days. Each point in this Figure corresponds to the RMS values calculated
430 for the HPP3.1 instruments S1.1, S1.2, S1.3.
431 We find that the 1 ppm accuracy threshold is met (and even surpassed) when measuring dried
432 air and for calibration intervals no longer than 6 days. We also see a marked difference between
433 the performances of each sensor: S1.1 shows the best performance, followed by S1.3 and S1.2.
434 The larger mean variation of ΔCO_2 (±4 ppm for S1) are observed for 19 days between two
435 calibrations. Surprisingly, one calibration each 45 days does not deteriorate the mean of ΔCO_2
436 significantly. Indeed, the variability of mean ΔCO_2 decreases over longer time periods as the
437 instruments do not have a residual no persistent long-term drift and positive and negative values
438 of ΔCO_2 cancel each other over time. The RMS of the minute averages slowly increases with
439 increasing calibration intervals but seems to stabilize between 3 and 4 ppm.

Atmos. Meas. Tech. Discuss., https://doi.org/10.5194/amt-2018-329
Manuscript under review for journal Atmos. Meas. Tech.
Discussion started: 4 October 2018

Atmospheric Measurement Techniques Discussions

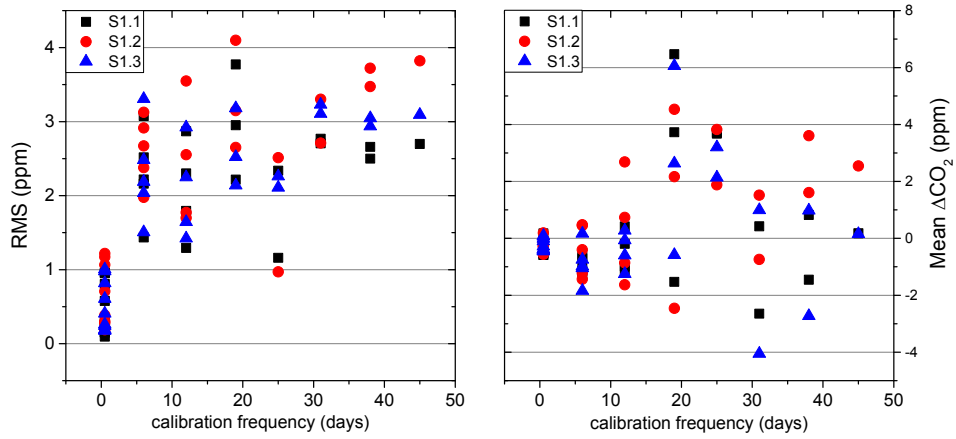

Figure 8: RMS (left) and mean difference (right) of CO_2 of the three HPP3.1 instruments compared to an independent accurate CRDS Picarrro, during a measurement period of 48 days. The x-axis represents different chosen frequencies for calibration of the HPP3.1 using reference cylinders.

4.2.2. Saclay ambient air measurements (test WA2-1)

During this test (section 3.3, *Saclay site*), all atmospheric variables in wet air which affect the performance of the instruments, i.e. pressure, temperature, water vapor content and CO_2 mixing ratios, were measured. As described in section 3.1, a six term multivariate linear regression is used to calculate the regression coefficients for each HPP3.2 instruments. Panel of Figure 9 shows the results for measurements from July 20th until August 8th 2016 of ambient air at Saclay from instrument HPP3.2 S2.2.

To illustrate the relative impact of the sensitivity to each variable on the reported raw data of CO_2 measurements each component of the multi-linear fit is added separately (one at a time here). Overall, we show 5 correction variables starting from the offset correction, in which only the offset of the regression is corrected until to the last panel in which all five terms of equation 1 are taken into account. The offset and concentration dependent corrections terms (b and $a_c x_c$) are the most significant corrections among all 5 parameters and allow reducing the mean ΔCO_2 from 45 ppm to 0 ppm. The other 4 parameters (pressure, temperature, water vapor and drift corrections) further reduce the difference between CRDS and HPP3.2 reducing the RMS of minute averages from 1.03 ppm to 0.67 ppm. Here, the temperature correction (d) and the water vapor correction (e) provide a correction of similar magnitude, keeping the same RMS and improving mean ΔCO_2 only from 0.16 to 0.13 ppm. This is understandable since temperature and water vapor are correlated for this type of measurement.

Atmos. Meas. Tech. Discuss., https://doi.org/10.5194/amt-2018-329
Manuscript under review for journal Atmos. Meas. Tech.
Discussion started: 4 October 2018

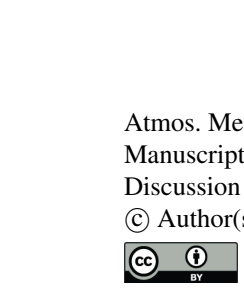

Atmospheric Measurement Techniques Discussions

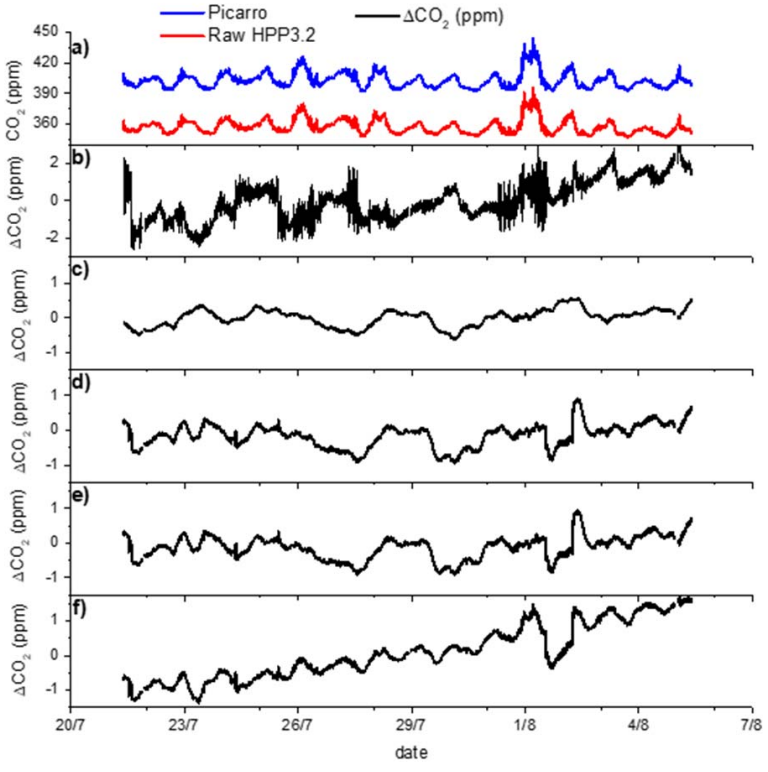

468

469 ***Figure 9:*** A continuous time series of 1 min averages for HPP3.2 instrument S2.2 compared to
470 the Picarro CRDS instrument after correcting for the different variables for a period of 15 days.
471 Plot (a) shows raw CO_2 measured by S2.2 and the Picarro. Plot (b) shows the difference
472 between Picarro and S2.2 after offset correction. The next 4 plots (c), (d), (e), (f) show the
473 difference to plot (b) after having correcting the HPP3.2 CO_2 to fit the Picarro CO_2 using
474 pressure, temperature, water vapor, and linear drift respectively. RMS and mean values of ΔCO_2
475 ($[CO_2]_{picarro}$ - $[CO_2]_{S2.2}$) data after each correction are shown in Table 3.

476

	raw	Offset correction	Pressure correction	Temperature correction	RH correction	Drift correction
RMS (ppm)	1.11	1.03	1.00	0.97	0.97	0.67
Mean (ppm)	45.33	1.0 10-3	8.6 10-4	0.16	0.13	-0.08

Atmos. Meas. Tech. Discuss., https://doi.org/10.5194/amt-2018-329
Manuscript under review for journal Atmos. Meas. Tech.
Discussion started: 4 October 2018

Atmospheric Measurement Techniques Discussions

Table 3: RMS and mean values of one minute average ΔCO_2 ($[CO_2]_{picarro}$] - $[CO_2]_{S2.2}$) data for each correction step. Note that corrections are cumulative from left to right.
A second instrument was deployed but the acquisition failed for a period of one week leading to a discontinuity in the data.

The laboratory studies (section 4.2.2.) already indicated that recalibration of the HPPs is required because of sensitivities to T, P and water vapor that are instrument-specific. We call the period during which the six calibration coefficients of Eq. (1) are calculated by fitting the PIcarro CO_2 time series, the learning period. Attempting to determine those calibration coefficients during a short learning period e.g. of one week, leads to high mean ΔCO_2, as can be seen in Figure 10. A learning period of two weeks leads to significantly better results. We tested systematically longer learning periods, of up to 45 days. The raw measurement data not used in the learning period is calibrated and compared to the CRDS system which then aids as a tool to assess the performance of this CO_2 calibration approach.
We also compared different learning periods of the same length. As an example, considering a 45 days experiment, we chose 3 different learning periods of successive 15 days. We also tested the approach of using the first and last weeks of a 45 days period to create a non-successive two weeks learning period.
Figure 10 shows the RMS and mean ΔCO_2 values considering 3 learning periods (C1, C2, C3) of 15 days each. The regression coefficients of the multilinear model of Eq. (1) for C1, C2 and C3 are calculated using the first, second and third consecutive 15 days of the experimental period. These coefficients are then used to predict corrected $[CO_2]_{HPP3.2}$ for the three cross-validation periods of 15, 30 and 45 days. Also, calibration coefficients (W1, W6) were calculated using the first and sixth week of the 45 days period for learning. Unsurprisingly, using C1 coefficients gives the best results for the first 15 days used for training (RMS=0.6 ppm and mean=-0.1 ppm for hourly values), and lead a higher bias for the last 15 days (RMS=1 ppm and mean=-1 ppm for hourly values). Using C2 coefficients to correct adjacent 15 days from the learning period gives comparable results (RMS=0.7, mean=-0.6 ppm and RMS=0.7, mean=-0.1 ppm respectively for the first and last 15 days). Considering the last learning period, C3 coefficients show a mean bias of -2.5 ppm when learning is from the first 15 days. One reason that can explain this behavior is the greater variability of CO_2 mixing ratio during the last 15 days of the experiment. The interquartile range of CO_2 mixing ratio is 10, 15 and 25 ppm respectively for the first, second and third period. The CO2 mixing ratio correction is accomplished mostly by correcting T, P, H_2O and the instrument offset. A small variation of sensitivities may lead to a less appropriate correction for periods of smaller variability. Another reason for this difference is the drift component of the correction in Eq. 1. The linear drift of the instrument also varies with time. One method to better correct for the slow linear drift of the instrument is to combine the first and last week of the experiment into a learning period instead of using two consecutive weeks. Figure 11 shows corrected ΔCO_2 ($[CO_2]_{picarro}$] - $[CO_2]_{HPP3.2}$) of S2.2 during 45 days when using this approach. When using the first week (W1) and the last week (W6) for learning, the instrument drift is not properly corrected and a residual slope of 0.14 and 0.28 ppm/week is shown in the black (W1) and the red (W6) curves of the figure, respectively. Nearly no drift (0.01 ppm/week) is observed when considering both W1 and W6 for the training (blue curve). On Figure 10, magenta stars show RMS and mean ΔCO_2 values of the whole 45 day time series considering both W1 and W6 as learning periods. With this coefficient determination method, mean ΔCO_2 bias can be reduced to nearly 0 ppm. Finally, averaging the 1-minute HPP3.2 data to hourly averages can further improve RMS values up to 28%. As expected, mean values do not change for hourly averages.

Atmos. Meas. Tech. Discuss., https://doi.org/10.5194/amt-2018-329
Manuscript under review for journal Atmos. Meas. Tech.
Discussion started: 4 October 2018

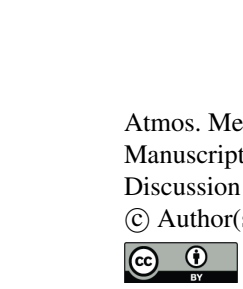

Atmospheric Measurement Techniques Discussions

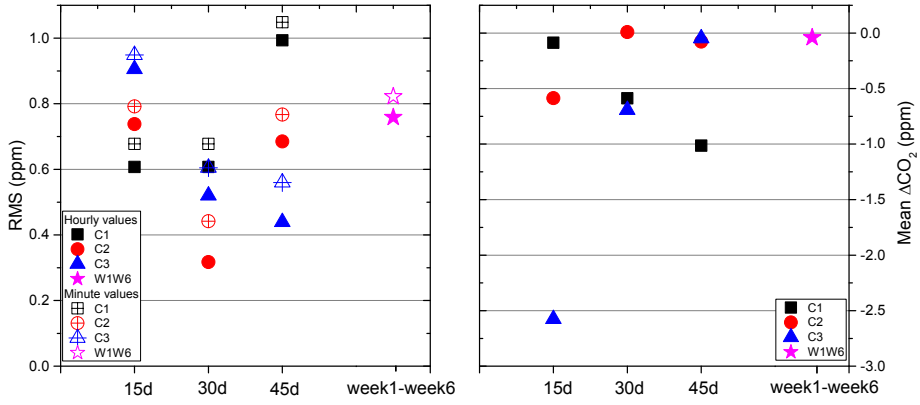

Figure 10: left – RMS values considering 3 learning periods of 15 consecutive days each in x-axis. C1, C2 and C3 correspond to RMS calculated considering correction coefficients determined from learning, that is, fitting of Eq. 1 to Picarro data during the first, second and third 15 consecutive days respectively. Week1-Week6 corresponds to RMS calculated considering correction coefficients determined during the first and last weeks of the experiment. Hourly and minute values are represented in full and empty symbols respectively. Right – Mean ΔCO_2 calculated for the four learning periods choices.

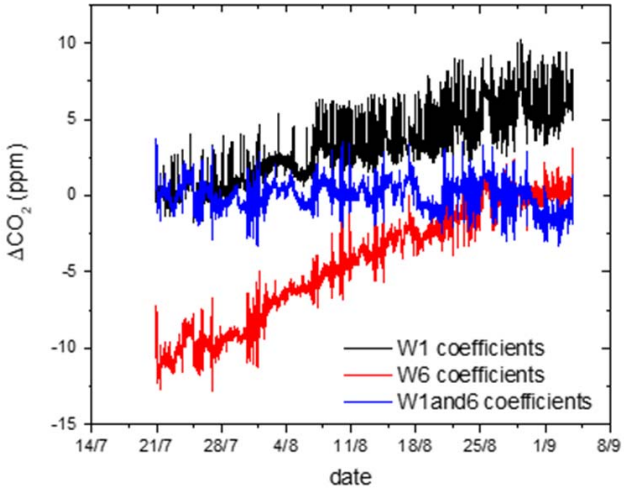

Figure 11: ΔCO_2 ($[CO_2]_{picarro}$ - $[CO_2]_{HPP3.2}$) of HPP3.2 instrument S2.2 during 45 days considering different learning periods of one week. Results from learning periods of week one (W1) and

Atmos. Meas. Tech. Discuss., https://doi.org/10.5194/amt-2018-329
Manuscript under review for journal Atmos. Meas. Tech.
Discussion started: 4 October 2018

Atmospheric Measurement Techniques Discussions

week six (W6) are in black and red respectively. The blue curve shows corrected ΔCO_2 when both W1 and W6 are used in the learning.

4.2.3. Urban site of Jussieu (test WA2-2)

To assess the performance of the HPP3.2 instruments, wet ambient air measurements at the urban site of Jussieu were carried for 60 consecutive days using HPP3.2 instrument S2.1 alongside a Picarro upon which learning is applied. Figure 12 shows RMS and mean values calculated with four learning periods of 15 consecutive days each and one learning considering both first and last week of the experiment. Calibration coefficients for C1, C2, C3 and C4 are calculated considering learning periods of first, second, third and fourth 15 consecutive days of the experiment respectively. W1W8 coefficients are calculated considering week one (W1) and week eight (W8) of the experiment.

First, we look at the results using C1, C2, C3 and C4 coefficients. Out of the four consecutive 15 day learning periods, C1 coefficients seem to provide the best correction of raw CO_2 mixing ratio with hourly RMS values between 0.3 and 0.6 ppm and mean values between 0 and 1 ppm. Absolute mean values of ΔCO_2 for C3 and C4 show a linear increase (slopes of 1.3 ppm per 15 days for C3 and 1.9 ppm per 15 days for C4) the further we go from learning periods leading to hourly mean values of -3.4 and -5.4 ppm respectively for C3 and C4 corrections. This is a typical case where the drift component could not be well characterized by the chosen learning periods. Another interesting observation concerns minute RMS values of C3 and C4 corrections which are lower than hourly RMS values for the same coefficients calculated during the first and second 15 days. Minute RMS are 0.1 and 0.4 ppm lower respectively for the first and second 15 day period for both C3 and C4 corrections. As for the previous urban measurements, considering both first and last weeks as a learning period provides satisfying results (RMS=1.1 ppm, mean=0.9 ppm) for the correction of raw CO_2 mixing ratios during a period of a month and a half.

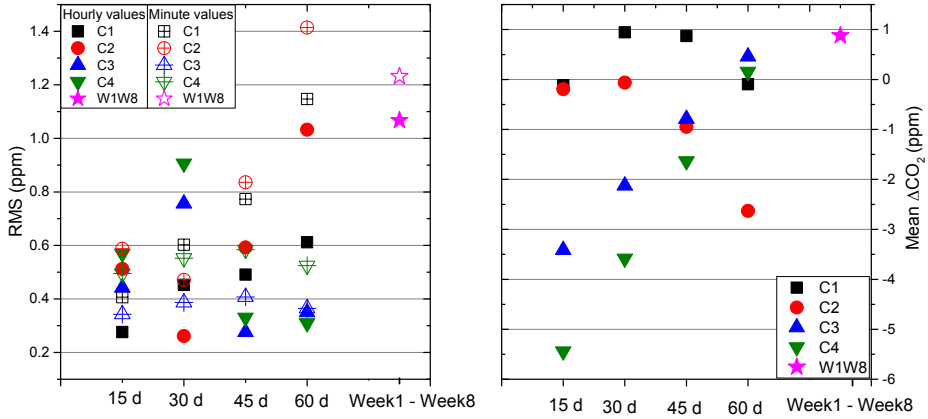

Figure 12: left – RMS values considering 4 learning periods of 15 consecutive days each. C1, C2, C3 and C4 corresponds to RMS calculated considering correction coefficients determined during the first, second and third 15 consecutive days respectively. W1W8 correspond to RMS calculated considering correction coefficients determined during the first and eighth weeks of the

experiment. Hourly and minute values are represented in full and empty symbols respectively. Right – Mean ΔCO_2 calculated with the same five coefficients mentioned above.

5. Conclusion and perspective

We integrated HPP3.1 and HPP3.2 NDIR sensors into a portable low-cost instrument with additional sensors and internal data acquisition. The laboratory tests reveal a strong sensitivity of measured CO_2 mixing ratios to ambient air pressure for the HPP3.1 series and a significantly decreased sensitivity to pressure, even for the upgraded HPP3.2 sensors equipped with a P sensor and using a manufacturer P-correction. To achieve the required stability and accuracy for urban observations, instruments have to be corrected at regular intervals against data from a very accurate reference instrument to account for their cross-sensitivities to T, P, H_2O changes and electronic drift, unless those parameters could be controlled externally in the future. We found that commercially available P, T and RH sensors that are compatible with the chosen Raspberry Pi3 platform are sufficiently precise to use these parameters as predictors of the linear equation use to calibrate each HPP instrument against the very accurate reference instrument, a process called learning.

Two common modes of operations have been successfully tested i.e. using the low-cost medium precision instrument for either dried or undried gas streams. Our results indicate that using a dried gas stream does not improve measurement precision or stability compared to an undried gas streams provided that a multilinear regression model is used for calibration (learning), which accounts for all cross-sensitivities including to H_2O mixing ratio changes.

We furthermore find that sensor specific corrections are required and they should be considered time-dependent, e.g. by including a linear drift that only becomes more apparent for longer-term observations. Different calibration strategies were tested for the Saclay and Jussieu ambient air measurements based on reference CRDS systems, and their results evaluated against CRDS cross validation data that were not used for learning. Those sites exhibit the typical mixing ratio enhancement in urban GHG monitoring networks were LCMP instruments could be deployed in the future. Regular (6 weekly) re-calibrations are found to be appropriate to capture sensor linear drifts and changes in relevant cross-sensitivities, while not increasing the burden of performing calibration too often by transplanting the low cost instrument to measure CO2 in parallel with a CRDS. Learning periods of one week with parallel CRDS measurements, spaced by a 'free running' period of 45 days, was sufficient for the HPP data to be within 1 ppm of CRDS during that period. This calibration approach by learning can be an alternative to permanently deploying calibration gases for each individual sensor. Overall, the requirement of ca. 1ppm compatibility for hourly means CO_2 mixing ratios for a dense CO_2 monitoring network in Paris (Wu et al. 2016) was achieved and no significant long-term bias was detected.

The field tests at the Saclay and Jussieu station are being continued to see if the instrument performance deteriorates over its lifetime. Since the start of the test in 2015 until now multiple HPP3.1 sensors have been in use for without significant performance loss.

Future improvements for the LCMP instruments will include the addition of batteries to allow their transport to the central calibration lab without power cut as well as using them in field campaigns, e.g. landfills when connected to solar panels or small wind turbines. During future tests at sites without reference instruments, small pressurized gas containers (12l, minican, Linde Gas) will be used to regularly inject target gas to track the performance.

The overall operational cost of the new calibration scheme using a central laboratory and rotating the LCMP systems can also only be assessed after more extensive field deployment has been performed.

Acknowledgements

The work conducted here was partially funded through the LOCATION project of the Low Carbon City Laboratory and a SME-VOUCHER from climate-KIC (EIT) as well as the Chaire BridGES of UVSQ, CEA, Thales Alenia Space and Veolia S.A.

References

Andres, R. J., Boden, T. A., and Higdon, D.: A new evaluation of the uncertainty associated with CDIAC estimates of fossil fuel carbon dioxide emission, Tellus B, 66, 23616, doi:10.3402/tellusb.v66.23616, 2014.

Bréon, F. M., Broquet, G., Puygrenier, V., Chevallier, F., Xueref-Remy, I., Ramonet, M., Dieudonné, E., Lopez, M., Schmidt, M., Perrussel, O., and Ciais, P.: An attempt at estimating Paris area CO_2 emissions from atmospheric concentration measurements, Atmos. Chem. Phys., 15, 1707-1724, https://doi.org/10.5194/acp-15-1707-2015, 2015.

Broquet, G., Bréon, F.-M., Renault, E., Buchwitz, M., Reuter, M., Bovensmann, H., Chevallier, F., Wu, L., and Ciais, P.: The potential of satellite spectro-imagery for monitoring CO_2 emissions from large cities, Atmos. Meas. Tech. Discuss., https://doi.org/10.5194/amt-2017-80, in review, 2017.

Cambaliza, M. O. L., Shepson, P. B., Caulton, D. R., Stirm, B., Samarov, D., Gurney, K. R., Turnbull, J., Davis, K. J., Possolo, A., Karion, A., Sweeney, C., Moser, B., Hendricks, A., Lauvaux, T., Mays, K., Whetstone, J., Huang, J., Razlivanov, I., Miles, N. L., and Richardson, S. J.: Assessment of uncertainties of an aircraft-based mass balance approach for quantifying urban greenhouse gas emissions, Atmos. Chem. Phys., 14, 9029-9050, https://doi.org/10.5194/acp-14-9029-2014, 2014.

Eugster, W. and Kling, G. W.: Performance of a low-cost methane sensor for ambient concentration measurements in preliminary studies, Atmos. Meas. Tech., 5, 1925–1934, https://doi.org/10.5194/amt-5-1925-2012, 2012.

Gaynullin, B., Bryzgalov, M., Hummelgård C., and Rödjegard, H., "A practical solution for accurate studies of NDIR gas sensor pressure dependence. Lab test bench, software and calculation algorithm," *2016 IEEE SENSORS*, Orlando, FL, 2016, pp. 1-3. Doi: 10.1109/ICSENS.2016.7808828.

Holstius, D. M., Pillarisetti, A., Smith, K. R., & Seto, E. (2014). Field calibrations of a low-cost aerosol sensor at a regulatory monitoring site in California. *Atmospheric Measurement Techniques*, *7*(4), 1121-1131, https://doi.org/10.5194/amt-7-1121-2014, 2014.

Hummelgård, C., Bryntse, I., Bryzgalov, M., Henning, J.-Å., Martin, H., Norén, M., and Rödjegård, H.: Low-Cost NDIR Based Sensor Platform for Sub-Ppm Gas Detection, Urban Climate, 14, Part 3, 342–350, doi:10.1016/j.uclim.2014.09.001, 2015.

Kunz, M., Lavric, J. V., Gerbig, C., Tans, P., Neff, D., Hummelgård, C., Martin, H., Rödjegård, H., Wrenger, B., and Heimann, M.: COCAP: a carbon dioxide analyser for small unmanned aircraft systems, Atmos. Meas. Tech., 11, 1833-1849, https://doi.org/10.5194/amt-11-1833-2018, 2018.

668 Lauvaux, T., et al. (2016), High-resolution atmospheric inversion of urban CO_2 emissions during
669 the dormant season of the Indianapolis Flux Experiment (INFLUX), J. Geophys. Res. Atmos.,
670 121, 5213–5236, doi:10.1002/2015JD024473.
671
672 Liu, Z., He, C., Zhou, Y., and Wu, J.: How much of the world's land has been urbanized, really?
673 A hierarchical framework for avoiding confusion, Landscape Ecol., 29, 763–771,
674 doi:10.1007/s10980-014-0034-y, 2014.
675
676 Martin, C. R., Zeng, N., Karion, A., Dickerson, R. R., Ren, X., Turpie, B. N., and Weber, K. J.:
677 Evaluation and environmental correction of ambient CO_2 measurements from a low-cost NDIR
678 sensor, Atmos. Meas. Tech., 10, 2383-2395, ttps://doi.org/10.5194/amt-10-2383-2017, 2017.
679
680 Mays, K. L., Shepson, P. B., Stirm, B. H., Karion, A., Sweeney, C., & Gurney, K. R. (2009).
681 Aircraft-based measurements of the carbon footprint of Indianapolis. Environmental Science and
682 Technology, 43(20), 7816-7823. DOI: 10.1021/es901326b.
683
684 Nassar, R., Hill, T. G., McLinden, C. A., Wunch, D., Jones, D. B. A., & Crisp, D. (2017).
685 Quantifying CO_2 emissions from individual power plants from space. Geophysical Research
686 Letters, 44, 10,045–10,053. https://doi.org/10.1002/2017GL074702.
687
688 Piedrahita, R., Xiang, Y., Masson, N., Ortega, J., Collier, A., Jiang, Y., Li, K., Dick, R. P., Lv, Q.,
689 Hannigan, M., and Shang, L.: The next generation of low-cost personal air quality sensors for
690 quantitative exposure monitoring, Atmos. Meas. Tech., 7, 3325–3336,
691 https://doi.org/10.5194/amt-7-3325-2014, 2014.
692
693 Raspberry Pi Foundation: Raspberry Pi Hardware Documentation, available at:
694 https://www.raspberrypi.org/documentation/hardware/raspberrypi/
695
696 Rella, C. W., Chen, H., Andrews, A. E., Filges, A., Gerbig, C., Hatakka, J., Karion, A., Miles, N.
697 L., Richardson, S. J., Stein-bacher, M., Sweeney, C., Wastine, B., and Zellweger, C.: High
698 accuracy measurements of dry mole fractions of carbon dioxide and methane in humid air,
699 Atmos. Meas. Tech., 6, 837–860, doi:10.5194/amt-6-837-2013, 2013.
700
701 Seto, K. C., Dhakal, S., Bigio, A., Blanco, H., Delgado, G. C., Dewar, D., Huang, L., Inaba, A.,
702 Kansal, A., Lwasa, S., McMahon, J. E., Müller, D. B., Murakami, J., Nagendra, H., and
703 Ramaswami, A.: Human settlements, infrastructure and spatial planning, in: Climate Change
704 2014: Mitigation of Climate Change. Contribution of Working Group III to the Fifth Assess-
705 ment Report of the Intergovernmental Panel on Climate Change, edited by: Edenhofer, O.,
706 Pichs-Madruga, R., Sokona, Y., Farahani, E., Kadner, S., Seyboth, K., Adler, A., Baum, I., Brun-
707 ner, S., Eickemeier, P., Kriemann, B., Savolainen, J., Schlömer, S., von Stechow, C., Zwickel,
708 T., and Minx, J. C., Cambridge, United Kingdom and New York, NY, USA, 2014.
709
710 Staufer, J., Broquet, G., Bréon, F.-M., Puygrenier, V., Chevallier, F., Xueref-Rémy, I.,
711 Dieudonné, E., Lopez, M., Schmidt, M., Ramonet, M., Perrussel, O., Lac, C., Wu, L., and Ciais,
712 P.: The first 1-year-long estimate of the Paris region fossil fuel CO_2 emissions based on
713 atmospheric inversion, Atmos. Chem. Phys., 16, 14703-14726, https://doi.org/10.5194/acp-16-
714 14703-2016, 2016.
715
716 Turner, A. J., Shusterman, A. A., McDonald, B. C., Teige, V., Harley, R. A., and Cohen, R. C.:
717 Network design for quantifying urban CO2 emissions: assessing trade-offs between precision

718 and network density, Atmos. Chem. Phys., 16, 134650013475, https://doi.org/10.5194/acp-16-
719 13465-2016, 2016.
720
721 Verhulst, K. R., Karion, A., Kim, J., Salameh, P. K., Keeling, R. F., Newman, S., Miller, J., Sloop,
722 C., Pongetti, T., Rao, P., Wong, C., Hopkins, F. M., Yadav, V., Weiss, R. F., Duren, R. M., and
723 Miller, C. E.: Carbon dioxide and methane measurements from the Los Angeles Megacity
724 Carbon Project – Part 1: calibration, urban enhancements, and uncertainty estimates, Atmos.
725 Chem. Phys., 17, 8313-8341, https://doi.org/10.5194/acp-17-8313-2017, 2017.
726
727 Wang, Y., Li, J. Y., Jing, H., Zhang, Q., Jiang, J. K., and Biswas, P.: Laboratory Evaluation and
728 Calibration of Three Low- Cost Particle Sensors for Particulate Matter Measurement, Aerosol
729 Sci. Tech., 49, 1063–1077, https://doi.org/10.1080/02786826.2015.1100710, 2015.
730
731 Wu, L., Broquet, G., Ciais, P., Bellassen, V., Vogel, F., Chevallier, F., Xueref-Remy, I., and
732 Wang, Y.: What would dense atmospheric observation networks bring to the quantification
733 of city CO2 emissions?, Atmos. Chem. Phys., 16, 7743–7771, https://doi.org/10.5194/acp-16-
734 7743-2016, 2016.
735
736 Young, D. T., Chapman, L., Muller, C. L., Cai, X. M., and Grimmond, C. S. B.: A Low-Cost
737 Wireless Temperature Sensor: Evaluation for Use in Environmental Monitoring Applications, J.
738 Atmos. Ocean. Tech., 31, 938–944, https://doi.org/10.1175/jtech-d-13-00217.1, 2014.